Ferroelectric Alignment of NLO Chromophores in Layered Inorganic Lattices: Structure of a Stilbazolium Metal−Oxalate from Powder Diffraction Data

John S. O. Evans,*[,†] Sophie Bénard,[‡] Pei Yu,[‡] and René Clément[‡,§]

Department of Chemistry, University of Durham, Science Laboratories, South Road, Durham, DH1 3LE, United Kingdom, and Laboratoire de Chimie Inorganique, U.M.R. 8613, Universite Paris Sud, 91405 Orsay Cedex, France

Received June 25, 2001
Revised Manuscript Received August 28, 2001

There has been considerable research over recent decades into organic materials displaying large second-order optical nonlinearities (NLO behavior).[1,2] Such materials are of potential use in second harmonic generation (SHG) and electrooptic[3] (EO) devices, which are of potential importance in areas such as optical communications and data storage. The area has been extensively reviewed.[4,5] Particular interest has been applied to stilbazolium-type chromophores, which have significant molecular hyperpolarizability (Figure 1). A prerequisite for bulk NLO activity is that the chromophores are arranged in a noncentrosymmetric fashion. The majority of chromophores of potential interest are, however, found to crystallize in centrosymmetric space groups. Considerable effort has therefore been applied to produce acentric chromophore arrangements using both chemical and physical control. Chemical techniques include the use of chiral species,[6] which by definition must adopt a noncentrosymmetric space group, the use of asymmetric hydrogen-bonding interactions,[7] the use of a variety of counterions in salts of chromophores,[8] the inclusion of chromophores in microporous materials such as zeolites,[9−14] and recently novel molecular self-assembly approaches for producing polar multilayered materials.[15−19] Physical techniques used have included cooling chromophores in a glassy matrix and applied field from above the glass transition temperature and incorporation of chromophores into Langmuir−Blodgett films.[20]

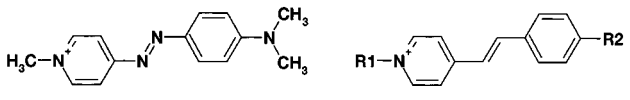

1 2

Figure 1. Cationic chromophores mentioned in the text. **1** = DAZOP, **2** = DAMS (R1 = Me, R2 = NMe_2); DAPS (R1 = isopropyl, R2 = NMe_2); MIPS (R1 = isopentyl, R2 = OMe).

One of us has previously shown that an alternative method of aligning chromophores is to include them in a suitable layered inorganic matrix. In this manner it may prove possible to prepare so-called "multifunctional materials" where the NLO properties of the chromophores coexist with, for example, conduction or magnetic properties of the host lattice. For example, the DAMS (see Figure 1) intercalate of the layered solid $MnPS_3$, $(DAMS)_{2x}[Mn_{1-x}PS_3]$, showed a second harmonic generation (SHG) efficiency at 1.34 μm, some 750 times that of urea combined with a spontaneous magnetization below 40 K.[21−24] In this material it appears that, despite the centric nature of the host lattice, the intercalated chromophores pack in a noncentrosymmetric fashion forming so-called J-type aggregates with a significant hyperpolarizability. It has also been reported recently that various stilbazolium chromophores can be included between metal−oxalate slabs of general formula $[M(II)M'(III)(ox)_3]^-$ (ox = $C_2O_4^{2-}$) to produce NLO active materials.[25] In addition to allowing influence over chromophore alignment, these inorganic:organic hybrids offer a second possibility for combining NLO properties and ferromagnetism in a single material. A number of other interesting materials based on layered oxalates have been described in the literature.[26−30]

* To whom correspondence should be addressed. Fax: (+44)191-384-4737. E-mail: john.evans@durham.ac.uk.
† University of Durham.
‡ Universite Paris Sud.
§ E-mail: rclement@icmo.u-psud.fr.

(1) Zyss, J. *Molecular Nonlinear Optics*; Academic Press: New York, 1994.
(2) Marder, S. R. In *Inorganic Materials*, 2nd ed.; O'Hare, D., Bruce, D. W., Eds.; John Wiley: Chichester, 1996.
(3) Dalton, L. R.; Steier, W. H.; Robinson, B. H.; Zhang, C.; Ren, A.; Garner, S.; Chen, A. T.; Londergan, T.; Irwin, L.; Carlson, B.; Fifield, L.; Phelan, G.; Kincaid, C.; Amend, J.; Jen, A. *J. Mater. Chem.* **1999**, *9*, 1905−1920.
(4) Burland, D. M. *Chem. Rev.* **1994**, *94*, 1−2.
(5) Denning, R. G. *J. Mater. Chem.* **2001**, *11*, 19−28.
(6) Andreu, R.; Malfant, I.; Lacroix, P. G.; Cassoux, P.; Roque, K.; Manoury, E.; Daran, J. C.; Balavoine, G. G. A. *C. R. Acad. Sci., Ser. IIc* **1999**, *2*, 329−340.
(7) Lacroix, P. G.; Daran, J. C.; Nakatani, K. *Chem. Mater.* **1998**, *10*, 1109−1114.
(8) Marder, S. R.; Perry, J. W.; Yakymyshyn, C. P. *Chem. Mater.* **1994**, *6*, 1137−1147.
(9) Cox, S. D.; Gier, T. E.; Stucky, G. D. *Chem. Mater.* **1990**, *2*, 609−619.
(10) Cox, S. D.; Gier, T. E.; Stucky, G. D.; Bierlein, J. *J. Am. Chem. Soc.* **1988**, *110*, 2986−2987.
(11) Werner, L.; Caro, J.; Finger, G.; Kornatowski, J. *Zeolites* **1992**, *12*, 658−663.
(12) Reck, G.; Marlow, F.; Kornatowski, J.; Hill, W.; Caro, J. *J. Phys. Chem.* **1996**, *100*, 1698−1704.
(13) Fyfe, C. A.; Brouwer, D. H. *Microporous Mesoporous Mater.* **2000**, *39*, 291−305.
(14) Marlow, F. *Molecular Crystals and Liquid Crystals* **2000**, *341*, 1093−1098.
(15) Katz, H. E.; Wilson, W. L.; Scheller, G. *J. Am. Chem. Soc.* **1994**, *116*, 6636−6640.
(16) Katz, H. E.; Scheller, G.; Putvinski, T. M.; Schilling, M. L.; Wilson, W. L.; Chidsey, C. E. D. *Science* **1991**, *254*, 1485−1487.
(17) Li, D. Q.; Ratner, M. A.; Marks, T. J.; Zhang, C. H.; Yang, J.; Wong, G. K. *J. Am. Chem. Soc.* **1990**, *112*, 7389−7390.
(18) Hanken, D. G.; Naujok, R. R.; Gray, J. M.; Corn, R. M. *Anal. Chem.* **1997**, *69*, 240−248.
(19) Lin, W. B.; Lin, W. P.; Wong, G. K.; Marks, T. J. *J. Am. Chem. Soc.* **1996**, *118*, 8034−8042.
(20) Prasad, P. N.; Williams, D. J. *Introduction to Nonlinear Optical Effects in Molecules and Polymers*; Wiley: New York, 1990.
(21) Clement, R.; Lacroix, P. G.; O'Hare, D.; Evans, J. *Adv. Mater.* **1994**, *6*, 794−797.
(22) Coradin, T.; Clement, R.; Lacroix, P. G.; Nakatani, K. *Chem. Mater.* **1996**, *8*, 2153−2158.
(23) Lacroix, P. G.; Lemarinier, A. V. V.; Clement, R.; Nakatani, K.; Delaire, J. A. *J. Mater. Chem.* **1993**, *3*, 499−503.
(24) Lacroix, P. G.; Clement, R.; Nakatani, K.; Zyss, J.; Ledoux, I. *Science* **1994**, *263*, 658−660.
(25) Benard, S.; Yu, P.; Audiere, J. P.; Riviere, E.; Clement, R.; Guilhem, J.; Tchertanov, L.; Nakatani, K. *J. Am. Chem. Soc.* **2000**, *122*, 9444−9454.
(26) Coronado, E.; Clemente-Leon, M.; Galan-Mascaros, J. R.; Gimenez-Saiz, C.; Gomez-Garcia, C. J.; Martinez-Ferrero, E. *J. Chem. Soc., Dalton Trans.* **2000**, 3955−3961.

10.1021/cm011155o CCC: $20.00
Published on Web 10/19/2001

In an initial study, some 35 phases of general formula $A[M(II)M'(III)(C_2O_4)_3]\cdot n(solvent)$ were prepared for a variety of M(II) [M = Mn, Fe, Co, Ni, Cu] cations with 7 different A chromophores (Figure 1).[25] Of these around two-thirds of the compounds showed NLO activity. Despite extensive efforts, however, it was only possible to grow single crystals, and therefore structurally characterize, two NLO inactive members of the family. Both these phases crystallized in the centrosymmetric space group $P2_1/c$, where the second-order susceptibility is necessarily zero. These materials thus present a frustrating dichotomy: the phases of least interest can be readily structurally characterized; those of most interest cannot.

There are clearly important factors controlling both the chromophore alignment in these materials and the ability to grow single crystals of sufficient size for structural characterization. To understand the origins of this control and to develop new or optimized materials, it is essential to have structural information for both the NLO active and inactive materials. In this communication we describe how this information has been obtained directly from powder diffraction data of an NLO active phase.

The synthesis of $DAZOP[MnCr(ox)_3]\cdot 0.5CH_3CN$ has been reported previously.[25] The material exhibits NLO activity ≈100 times that of urea at 1.9 μm and orders ferromagnetically at 6 K. Powder diffraction data were recorded on a sample of the material loaded in a 0.5-mm glass capillary on a Bruker d8 diffractometer.[31] The data could be indexed on a monoclinic cell of $a = 9.3251(4)$ Å, $b = 16.2931(9)$ Å, $c = 8.7103(3)$ Å, and $\beta = 82.893(3)°$. Systematic absences and a subsequent Pawley[32] model-independent fit to the diffraction data suggested the noncentrosymmetric space group $P2_1$.

For structure solution, a novel real-space simulated annealing[33] approach was used within the Topas suite of software.[34] The known layered metal−oxalates have structures based on octahedrally coordinated M(II) and M(III) ions held together by bridging oxalate groups in such a way as to produce a two-dimensional honeycomb layer. The scattering from the layers was therefore initially approximated by two rigid octahedral MO_6 groups, which were free to translate and rotate in two dimensions within the unit cell, but restricted to lie approximately coplanar (± 0.9 Å) and with their 3-fold axes approximately (±20°) parallel to the crystallographic c axis. The DAZOP molecule was included as a planar, rigid species allowed to rotate and translate in three dimensions, but constrained to lie approximately (±0.9 Å) midway between the inorganic layers. These groups model some 79% of the total scattering power. Simulated annealing cycles were then performed in which these three species were translated/rotated at random and their positions subsequently refined by the Rietveld method. An annealing protocol was adopted in which random shifts in group coordinates/rotations were scaled according to a specified "temperature" regime. This temperature was systematically varied during the solution cycles until the global minimum was located.

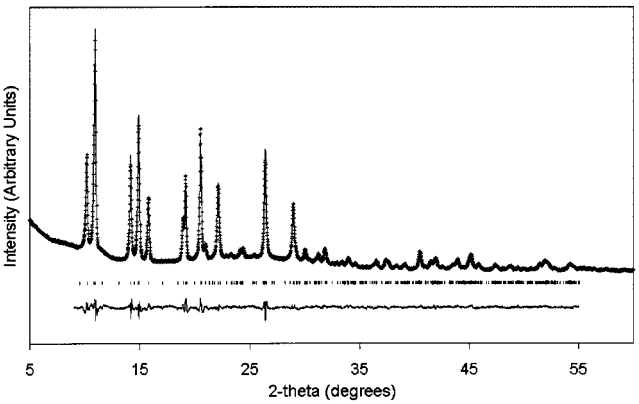

Figure 2. Final Rietveld plot for $DAZOP[MnCr(ox)_3]\cdot 0.6CH_3CN$. Observed data (small crosses), calculated curve (solid line), and difference curve (lower solid line) are shown. Small vertical tick marks show reflection positions allowed by symmetry.

After several thousand cycles of model refinement/perturbation, a reasonable agreement to the experimental data was achieved. From the relative orientations of MO_6 octahedra in the inorganic layer it was possible to infer likely positions of the carbon atoms of the oxalate ions. A second model was then developed in which oxalate ions were treated as three independent rigid groups with internal bond distances and angles derived from the Cambridge structural database.[35] A more flexible definition of the DAZOP molecule was developed in which torsion angles between the two rings and the central diazo N=N unit and between the NMe_2 group and the C_6H_4 ring were allowed to vary. A CH_3CN solvent molecule was also introduced as a rigid body with a variable occupancy. Several tens of thousands of cycles of model perturbation/Rietveld refinement were then performed during which the various rigid groups (DAZOP molecule, oxalate anions, and solvent) were allowed to vary their positions and orientations within the unit cell at random, subject to the restraints that the metal−oxalate layer network remained intact (M−O bonds forced to remain <2.3 Å), the DAZOP molecule remained approximately halfway between the metal−oxalate layers and the solvent remained at a nonbonded distance from other atoms.

In this manner a structural model that displayed excellent agreement with experimental data was achieved. Subsequent Rietveld refinement in which coordinates and angles of the various atoms and rigid groups, along with internal degrees of freedom of the DAZOP molecule and the solvent occupancy, were refined (62 variable parameters total[36]) gave the fit of Figure 2. Final agreement figures of wRp = 1.45% (8.4%

(27) Decurtins, S.; Schmalle, H. W.; Oswald, H. R.; Linden, A.; Ensling, J.; Gutlich, P.; Hauser, A. *Inorg. Chim. Acta* **1994**, *216*, 65−73.
(28) Martin, L.; Turner, S. S.; Day, P.; Guionneau, P.; Howard, J. A. K.; Hibbs, D. E.; Light, M. E.; Hursthouse, M. B.; Uruichi, M.; Yakushi, K. *Inorg. Chem.* **2001**, *40*, 1363−1371.
(29) Nuttall, C. J.; Day, P. *Chem. Mater.* **1998**, *10*, 3050−3057.
(30) Mathoniere, C.; Nuttall, C. J.; Carling, S. G.; Day, P. *Inorg. Chem.* **1996**, *35*, 1201−1206.
(31) Data for Rietveld refinement were collected on a sample packed in a 0.5-mm thin-walled glass capillary using a Bruker d8 diffractometer equipped with Cu Kα radiation, a Ge(111) incident beam monochromator, and a Braun linear position-sensitive detector. A 2θ range of 4°−90° with a step size of 0.0145° and a total time per step of 30 s was used.
(32) Pawley, G. S. *J. Appl. Crystallogr.* **1981**, *14*, 357−361.
(33) Coelho, A. A. *J. Appl. Crystallogr.* **2000**, *33*, 899−908.
(34) Bruker AXS Ltd.; Topas V2.0: General Profile and Structure Analysis Software for Powder Diffraction Data; Bruker AXS: Karlsruhe, 2000.
(35) Allen, F. H.; Kennard, O. *Chem. Des. Autom. News* **1993**, *8*, 31−37.

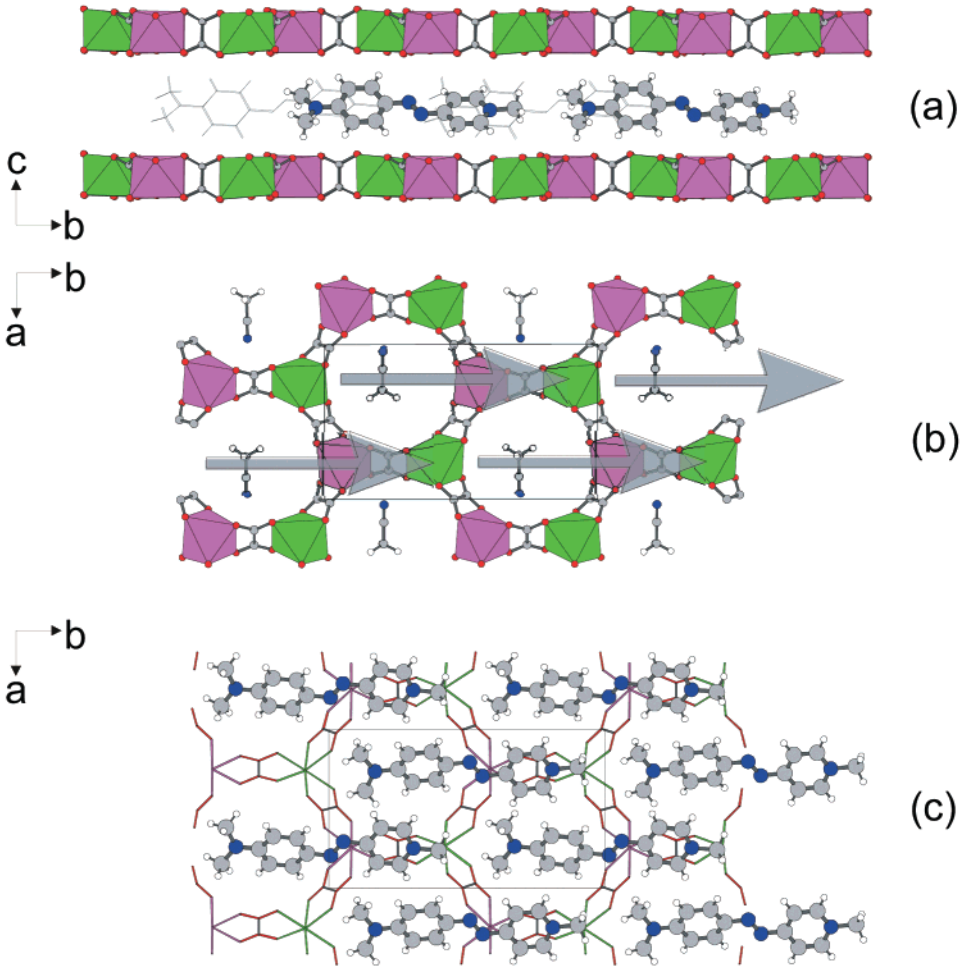

Figure 3. Structure of DAZOP[MnCr(ox)$_3$]·0.6CH$_3$CN. (a) A perspective view of the structure, (b) the metal−oxalate layers, and (c) the polar alignment of DAZOP chromophores within a single layer. In (b) the polar arrangement of guest molecules is emphasized by arrows. Carbon atoms, gray spheres; nitrogen, blue; hydrogen, white. MO_6 groups in (a) and (b) shown as solid octahedra.

with background subtracted) and $R_{Bragg} = 2.74\%$ were achieved. This represents a structure solution of a material containing 61 atoms in the asymmetric unit (44 non-H) from laboratory powder X-ray data.[37]

Views of the three-dimensional structure of DAZOP-[MnCr(ox)$_3$] are shown in Figure 3. The metal−oxalate layers form a honeycomb arrangement as expected (Figure 3b) with average metal−oxygen distances of 2.15 Å for the two metal sites. One would clearly expect Cr(III)−O distances to be considerably shorter than Mn-(II)−O distances. This suggests the metal atoms (which cannot otherwise be readily distinguished by X-ray measurements) are disordered over the two sites available. We presume that this disorder occurs along the stacking axis: Mn(II)/Cr(III) being ordered within individual two-dimensional sheets, but this order being lost between subsequent layers. Analogous disorder is found in MIPS[MnCr(ox)$_3$], though in DAPS[MnCr(ox)$_3$] ordered metal sites are found.[25] Individual oxalate layers are essentially planar, with none of the "waviness" exhibited by the DAPS/MIPS- containing materials.[25] Solvent molecules are located in the intralayer cavities, in positions similar to those of solvent molecules in related materials.

The polar alignment of DAZOP chromophores is emphasized in Figure 3c. Individual DAZOP molecules lie with their long axis approximately parallel to the crystallographic *b* axis and their molecular plane at ≈48° to the layers. The molecules are uniformly packed within the layers with distances between the mean molecular planes of 3.42 and 3.11 Å. The sensitivity of the diffraction data to internal torsion angles of the guest aromatic rings relative to the central N=N unit

(36) For final cycles of refinement a total of 62 parameters were refined: scale factor, 3 peak shape parameters, 10 background parameters, zero point, 4 cell parameters, 30 fractional coordinates and rotation angles for the 5 rigid groups, 3 internal torsion angles of the DAZOP molecule, 6 metal fractional coordinates, and a solvent occupancy. Three unique temperature factors were refined: one temperature factor for Cr/Mn sites, a second for atoms of oxalate groups, and a third for C/N atoms of the DAZOP molecule. Ring hydrogens were set to a value 20% higher than DAZOP C/N atoms and methyl hydrogens 50% higher. Data were refined over a 2θ range of 9°−55°; no significant features were discernible beyond this range.

(37) The sensitivity of powder X-ray data to the various parameters of this model was verified by Rietveld refinement of powder data collected on the centrosymmetric DAPS[MnCr(ox)$_3$], whose structure has been determined by single-crystal measurements.[25] These studies indicated that powder data are sufficiently sensitive to factors such as hydrogen atoms and solvent occupancy to warrant their inclusion in the final model. The solvent occupancy refined to 0.59(2), in good agreement with the experimental value of 0.5. The absence of significant preferred orientation effects for DAZOP[MnCr(ox)$_3$] was examined by also recording data in Bragg−Brentano (reflection) geometry; an excellent Rietveld fit was obtained to the data using the same structural model. To ensure that the model reported represents a global minimum, several hundred thousand cycles of model perturbation were performed in which the DAZOP molecule location and torsion angles were set to random values and allowed to undergo cycles of refinement/simulated annealing. In all cases the model presented here was the lowest *R*-factor solution obtained.

was investigated by systematically stepping torsion angles over a 0°−180° range and performing a full Rietveld refinement at each step (361 refinements total) and also to the torsion angle of the NMe_2 group. These refinements suggested the molecule is essentially planar with torsion angles of 5° ± 5° (C_6H_5NMe ring), 12° ± 5° (C_6H_4 ring), and 5° ± 6° (NMe_2 to C_6H_4 ring). Torsion angles of the seven compounds with central diazo units in the Cambridge structural database showed an rms deviation from planarity of 3°. In contrast, ring−ring dihedral angles of 13.3° and 30.8° are found for the centric DAPS and MIPS compounds, respectively.

The packing arrangement of DAZOP chromophores between individual oxalate layers will be determined by a number of factors. First, there is the need to maintain charge balance between the negatively charged layers and the positively charged chromophore molecules. This will determine the overall chromophore packing density. For a relatively high packing density, as necessitated by the layer charge, the rodlike shape of these chromophores will make a parallel arrangement extremely likely. Second, the tilting of the molecular plane of DAZOP will reduce the mean DAZOP-layer separation, increasing DAZOP-layer electrostatic contributions. The tilting level adopted leads to a relatively uniform packing in two dimensions. Finally, DAZOP molecules are shifted relative to one another in such a way that the donor moieties of one chromophore lie next to acceptor moieties of that adjacent, maximizing DAZOP−DAZOP electrostatic attractions. This combination of factors combines to produce polar individual chromophore layers. Very similar arrangements have been observed in related materials where cationic chromophores and anions segregate into "pseudo-layers" in the structure.[38,39]

The parallel alignment of each subsequent chromophore layer in the structure presumably arises from specific DAZOP-layer interactions dominating other factors, which might tend to align subsequent layers in a nonparallel or even antiparallel (resulting in an overall zero second-order susceptibility) fashion. These will be mediated by the structural rigidity of the oxalate layers. If one represents the structure schematically as AB(DAZOP)AB(DAZOP)..., where A and B refer to the surfaces of the oxalate layers, then factors favoring a specific chromophore arrangement within one layer will be naturally propagated through the material. However, given the pseudo 3-fold symmetry of the layers, one might expect that subsequent DAZOP layers could adopt any one of three orientations at 120° to an initial layer. For an ideal trigonal system one would expect a b/a ratio of $\sqrt{3}$ or 1.732. For DAZOP[$MnCr(ox)_3$] the b/a ratio is 1.746, which represents an ≈0.8% distortion from trigonal symmetry. This distortion is presumably sufficient to energetically discriminate one of these three orientations relative to the others, resulting in the collinear polar chromophore arrangement observed and bulk NLO activity.

The question then remains as to why the DAZOP chromophore adopts a noncentrosymmetric packing arrangement within the oxalate layers whereas others do not. Of the various A[M(II)M′(III)$(ox)_3$] phases prepared to date it is those with the smallest mean interlayer separation that exhibit the highest NLO activity. These are the materials in which the chromophore size and shape presumably match the layer size and charge density most closely. In fact, for the DAZOP case there is a natural registry between the chromophore length (≈15.9 Å) and the crystallographic b axis (16.3 Å). This leads to a densely packed arrangement (Figure 3c) in which each DAZOP molecule can adopt an essentially identical position with respect to the host layers, favoring the formation of a highly crystalline, ordered material. In the case of DAZOP these factors lead to the close interaction between adjacent chromophores, essentially planar chromophore molecules, and large specific layer−chromophore interactions—the factors which will favor a bulk polar structure. Preliminary evidence suggests that DAZOP[$FeCr(ox)_3$] and DAMS[$MnCr(ox)_3$] have closely related structures. Further work on these and related materials is in progress.

Supporting Information Available: A table of fractional atomic coordinates (PDF) and an X-ray crystallographic file (CIF) have been deposited. This material is available free of charge via the Internet at http://pubs.acs.org.

CM011155O

(38) Marder, S. R.; Perry, J. W.; Schaefer, W. P. *J. Mater. Chem.* **1992**, *2*, 985−986.
(39) Okada, S.; Ohsugi, M.; Masaki, A.; Matsuda, H.; Takaragi, S.; Nakanishi, H. *Mol. Cryst. Liq. Cryst.* **1990**, *183*, 81−90.